Joint PP/PS tomography with Dynamic Warping

Yang He, Guy Hilburn, Francis Sherrill (TGS)*

Summary

PS depth imaging requires a model that flattens events on both PP and PS common image gathers (CIGs) and images corresponding events at consistent depths for both data types. To satisfy these constraints we build an objective function consisting of measures of gather flatness, depth consistency, and well information if available. Both PP and PS gathers are flattened simultaneously, and to ensure depth consistency a floating event constraint is implemented by penalizing the relative depth shifts between PP and PS images. The depth shifts are measured by Dynamic Warping (DW) because it suffers less from cycle-skipping than local calculations by solving the problem of matching two images globally and optimally. With well information, tomographic inversion is able to derive anisotropic velocity models from PP and PS reflection seismic data efficiently and accurately. Tests on synthetic data and a 3D land data example illustrate the effectiveness of the joint PP/PS tomography with DW.

Introduction

Multicomponent seismology has played an important role in the oil exploration industry in recent years. PS waves can provide valuable information in reservoir characterization, such as lithological discrimination or estimation of rock properties. Also, as shear waves are less affected by attenuation than compressional waves, they can help in imaging of reservoirs beneath gas clouds (Stewart et al., 2003). S-waves are usually more sensitive to anisotropy than P-waves and can provide an additional constraint on anisotropy estimation (Tsvankin, 2012). Tsvankin and Grechka (2011) and Cai and Tsvankin (2012) state that when both horizontal and dipping interfaces exist, combining PP and PS moveout can resolve both the vertical velocities and anisotropy. PS waves may also image the subsurface better where PS reflectivity is stronger than PP. With all the benefits of PS waves, it is crucial to build correct models to take full advantage of the combined information from PP and PS waves. To this end, joint tomographic inversion of PP and PS data is an excellent choice for its efficiency and flexibility for combining all constraints, as discussed in several publications (Stopin and Ehinger, 2001; Broto et al., 2003; Foss et al., 2005; Liu et al., 2006; Szydlik et al., 2007). Our algorithm for updating the model parameters, vertical P-wave velocity (V_{P0}), vertical S-wave velocity (V_{S0}), and Thomsen anisotropic parameters (ε and δ), is based on the gridded reflection tomography conducted on post-migration CIGs. In addition to correcting residual moveout (RMO) in image gathers, the algorithm measures the depth shifts automatically by DW and penalizes depth misties between the migrated PP and PS images. The inclusion of PS data and requirement for depth consistency introduce extra constraints and provide better effective illumination for model building.

Method

First, we apply prestack Kirchhoff depth migration to generate PP and PS depth gathers. The initial model may be obtained from stacking velocity or well logging.

The objective function used in the joint tomography of PP- and PS waves is a linear combination of four components and is defined as follows:

$$E(\Delta m) = \alpha_1\|A_{PP}\,\Delta m + d_{PP}\|_2 + \alpha_2\|A_{PS}\,\Delta m + d_{PS}\|_2 + \alpha_3\|D\Delta m + d_{DW}\|_2 + \alpha_4\|\,W\Delta m + d_{well}\,\|_2$$

Δm is the calculated update of all model parameters, including velocities and anisotropic models. The first and second components are defined to flatten PP and PS wave CIGs by minimizing their RMO. The matrices A_{PP} and A_{PS} include the sensitivity of the PP and PS moveouts along the PP and PS rays with respect to the elements of the model parameters. The vectors d_{PP} and d_{PS} represent the RMO in PP and PS wave CIGs. The third piece of the objective function is included to enforce depth consistency. The matrix D describes the derivatives of the PP and PS migrated depth differences with respect to the model parameters, and the vector d_{DW} contains the shifts between the migrated depths on the PP and PS images, which can be obtained by DW. Well information may be included in the fourth component, derived from checkshots, sonic logging, or depth markers for geological layers. The coefficients α_1, α_2, α_3 and α_4 determine the weights of the corresponding terms. A regularization term and preconditioning can be included to help stabilize the inversion and improve convergence, but are not listed here for clarity.

PS waves can supplement PP waves with additional illumination because they sample different areas of the subsurface, providing more constraint and helping ensure the success of tomography. The additional requirement of codepthing provides redundant information for a more accurate and stable inversion. Though the inclusion of PS data and constraints on V_p/V_s ratio do not allow us to fully resolve the anisotropic parameter δ, they do help to resolve ε-δ, which is vital for S-wave propagation. If well information is available in the format of checkshots, sonic logging, or geological markers, the extra constraint allows us to resolve δ as well. Updating P-wave velocity, followed

DOI http://dx.doi.org/10.1190/segam2015-5916442.1

sequentially by updating S-wave velocity, may take a number of iterations to converge to a satisfactory velocity model. When anisotropic parameters are introduced, model building can be more complicated. We can reduce the required iterations by using joint PP/PS tomography to update all V_P, V_s, and anisotropic parameters simultaneously by utilizing all available data, including gather flatness, image misties, and well information.

Dynamic Warping

During PP and PS model building, any velocity errors can cause substantially incorrect positioning of PS data, which leads to misties with the PP image. The shift between the PP and PS images is built into the objective function to achieve codepthing. The conventional way to analyze the shift between PP and PS images is to manually interpret corresponding major events. This method requires tremendous human time and is almost impossible to perform for all reflectors. DW tries to match two images with minimal local dissimilarity automatically. The main strength of DW is in solving the minimization problem globally and optimally. Thus, the resulting shift estimates are much less prone to cycle-skipping errors and the algorithm tolerates complicated differences between base and monitor data sets. DW has been proven to be able to estimate displacements in time associated with the registration of PP and PS images (Hale 2013). In Figure 1, DW is applied to align a PS image to a PP image in depth. Between the original PS and PP images, we can see that the amplitude, bandwidth and phase are different. In the intermediate depth range, some reflectors visible on the PS image are weak on the PP image. The inherent differences between the two images complicate matching geological layers. With DW a smooth displacement field is estimated which shifts the left side of the PS image upward while pushing the right side downward. Overall, the undulations in the PS image are reduced to match the PP image. Therefore, it can be shown that DW measures the shifts between these PP and PS depth images accurately. The alignment of the PS image to the PP image is improved after warping. One major feature of DW is that it imposes constraints on the rate at which shifts may vary in time or depth, and these constraints enable accurate estimation of shifts from sequences that are contaminated with noise, and make the process less sensitive to cycle skipping. Venstad (2014) demonstrated that DW can accurately estimate large and rapidly varying shifts. It yields more accurate results than methods based on local cross correlation, especially when shifts vary over short spatial scales.

Well Information

There are usually three kinds of well information: checkshot, sonic logging, and well markers. Each provides velocity information in a different way. Checkshots

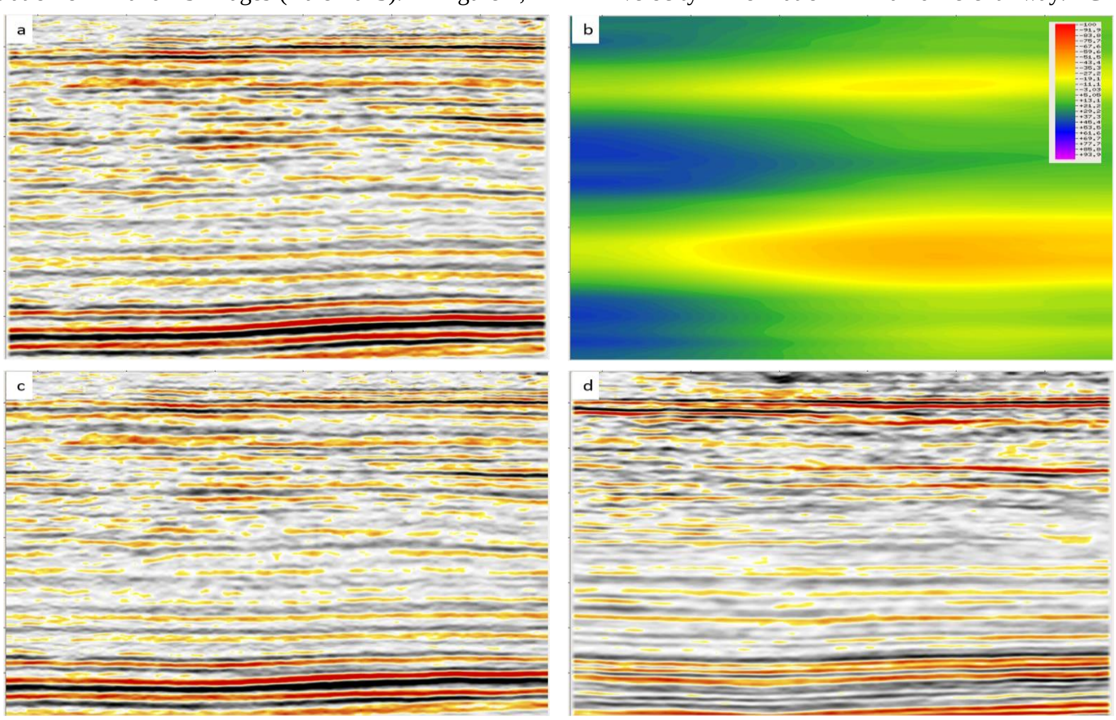

Figure 1: (a) PS image before warping. (b) The displacement estimated by DW. (c) PS image after warping. (d) PP image. PS image aligns better with PP image after applying the displacement.

DOI http://dx.doi.org/10.1190/segam2015-5916442.1

measure the first-arrival traveltimes from borehole to the surface to constrain the average velocity of the model. For VTI media, checkshots can be inverted for velocities along the (vertical) symmetric axis around the well. Sonic logging measures local interval velocity directly. Once the vertical velocity is known, it is simple to conduct anisotropy estimation. However, for a TTI case, tomography has to be performed in a well-tied form to resolve both velocity and anisotropy since checkshots and sonic logging only measure velocity along certain angles away from the symmetric axis. More often, well markers are provided as misties between a seismic image and wells. By comparing the depths of certain layers in the image and actual depths interpreted from log data, the differences are obtained and recorded as seismic-to-well misties. This is valuable for determining the correct velocity model and anisotropy. To update the model, a zero-angle ray is traced from the normal direction of the reflector, and the misties are back-projected along the ray path by conversion from depth to time. The well information is vital to reduce ambiguity and helps to decouple the velocity and anisotropy.

Synthetic Example

Synthetic data was generated to test the joint tomography. Kirchhoff PSDM was run on the synthetic vertical and radial components using a smooth initial model. The resulting PP and PS CIGs can be seen in Figure 2. Because the marker was used as constraints, the depth errors were reduced after inversion while gather flatness was improved.

A 3D Land Data Example

We demonstrate our method to perform joint PP/PS tomography on a 3D land data set, which was acquired at a central Alberta Canada field in 2014. The pre-stack time migration processing produced PS images that allowed successful detection of low PP impedance contrast layers. Depth processing of multicomponent seismic data is technologically challenging, and the imaging of PS data consistent with PP data represents one of the main difficulties. The initial models were built according to sonic logging which does not extend to the very shallow region. Uncertainty exists in the shallow that could introduce velocity errors. After initial migration there are significant errors in alignment between the PP and PS images. Substantial moveouts in the gathers suggest obvious errors in velocities, especially for the PP gathers. The shallow part of the land survey is not well illuminated because of the limitations in reflection angle. Thus the shallow reflectors are not imaged well. After joint tomography, the P velocity is increased in the shallow while the S velocity is reduced. The gather flatness is greatly improved and the PSDM results show enhanced coherency and good alignment between PP and PS images in Figure 3 and 4.

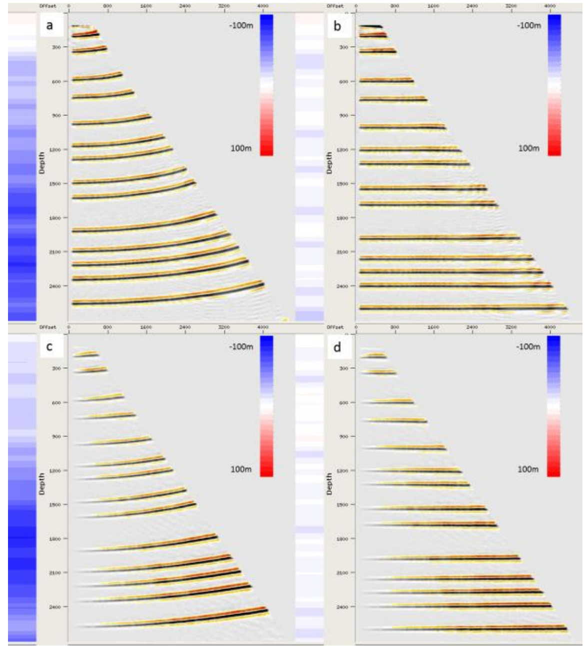

Figure 2: (a) and (c): initial PP and PS gathers. (b) and (d): PP and PS gathers after joint tomography. The corresponding shifts between migration depth and marker depth are plotted to the left of each gather in the same color scale.

Conclusions

Dynamic Warping is effective in estimating the relative shifts between PP and PS images in depth. The estimated shift can be used as an additional constraint for joint PP/PS tomography. The joint tomography is effective in flattening both PP and PS gathers while codepthing the corresponding events. With the inclusion of PS data, the anisotropic problem still can’t be fully resolved. But better illumination from PS waves gives more constraints for model building. With well information available, it also produces more accurate anisotropic models that tie to the wells.

Acknowledgements

The authors would like to thank Bin Wang, Zhiming Li, Connie VanSchuyver, and Christopher Egger for reviewing this paper and for helpful discussion. We also thank TGS’s Arcis office for providing the real data and time processing results. Appreciation is also extended to Feng Hao for help with the Dynamic Warping programming, as well as TGS management for permission to publish this paper.

DOI http://dx.doi.org/10.1190/segam2015-5916442.1

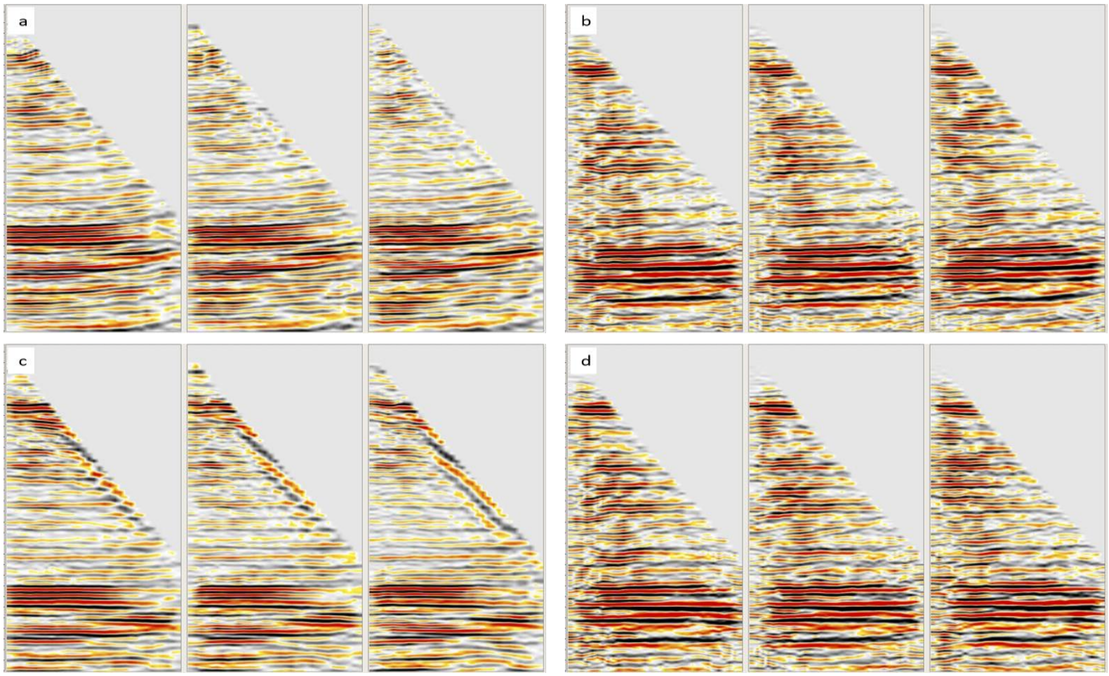

Figure 3: (a) and (b) initial PP and PS gathers. (c) and (d) PP and PS gathers after joint tomography.

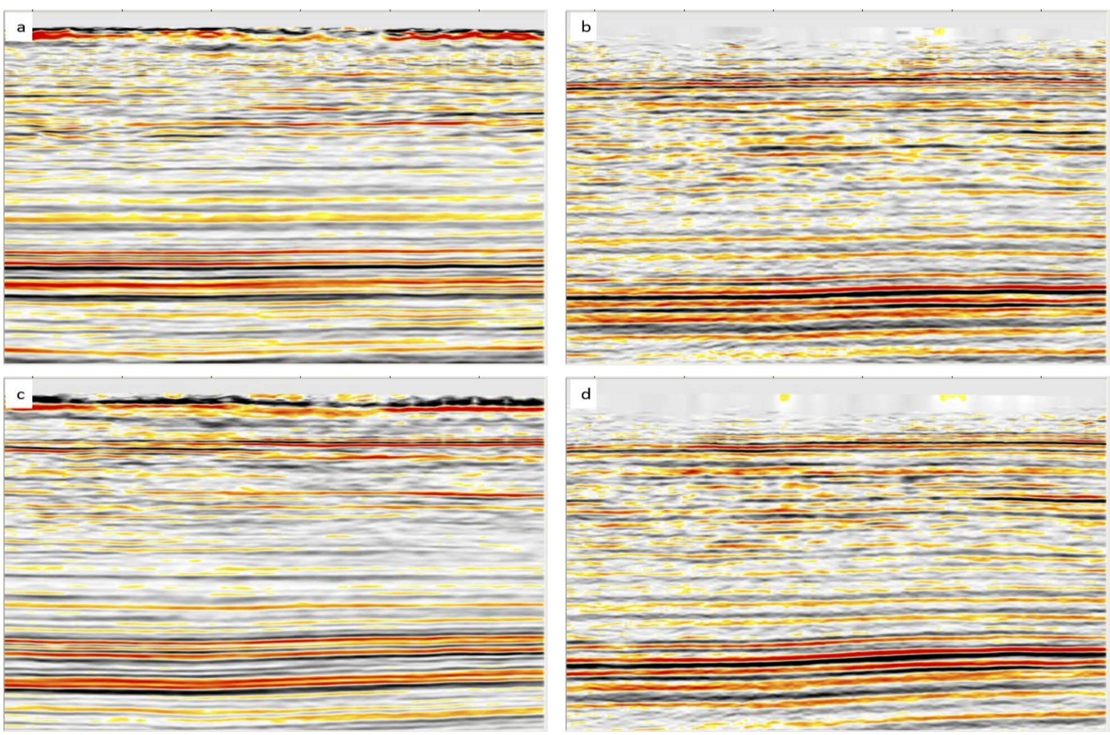

Figure 4: (a) and (b) initial PP and PS images. (c) and (d) PP and PS images after joint tomography.

DOI http://dx.doi.org/10.1190/segam2015-5916442.1

EDITED REFERENCES

Note: This reference list is a copyedited version of the reference list submitted by the author. Reference lists for the 2015 SEG Technical Program Expanded Abstracts have been copyedited so that references provided with the online metadata for each paper will achieve a high degree of linking to cited sources that appear on the Web.

REFERENCES

Broto, K., A. Ehinger, J. H. Kommedal, and P. G. Folstad, 2003, Anisotropic travel time tomography for depth consistent imaging of PP and PS data: The Leading Edge, **22**, 114–119. http://dx.doi.org/10.1190/1.1559037.

Cai, P., and I. Tsvankin, 2012, Joint migration velocity analysis of PP- and PS- waves for VTI media: 82nd Annual International Meeting, SEG, Expanded Abstracts. http://dx.doi.org/10.1190/segam2012-0873.1.

Foss, S.-K., B. Ursin, and M. V. de Hoop, 2005, Depth-consistent reflection tomography using PP and PS seismic data: Geophysics, **70**, no. 5, U51–U65. http://dx.doi.org/10.1190/1.2049350.

Liu, J., T. Jenkinson, A. Shatilo, L. Bear, and T. Rape, 2006, PS depth imaging and model building at Beryl; A 3D, 4-C OBC data set: 77th Annual International Meeting, SEG, Expanded Abstracts, 1029–1033. http://dx.doi.org/10.1190/1.2792579.

Hale, D., 2013, Dynamic warping of seismic images: Geophysics, **78**, no. 2, S105–S115. http://dx.doi.org/10.1190/geo2012-0327.1.

Stewart, R., J. Gaiser, R. Brown, and D. Lawton, 2003, Converted-wave seismic exploration: Applied Geophysics, **68**, no. 1, 40–57. http://dx.doi.org/10.1190/1.1543193.

Stopin, A., and A. Ehinger, 2001, Joint PP/PS tomographic inversion of the mahogany 2D 4C OBC seismic data: 71st Annual International Meeting, SEG, Expanded Abstracts, 837–840. http://dx.doi.org/10.1190/1.1816765.

Szydlik, T., P. Smith, S. Way, L. Aamodt, and C. Friedrich, 2007, 3D PP/PS prestack depth migration on the Volve field: First Break, **25**, no. 4.

Tsvankin, I., 2012, Seismic signatures and analysis of reflection data in anisotropic media, 3rd ed.: SEG References No 19.

Tsvankin, I., and V. Grechka, 2011, Seismology of azimuthally anisotropic media and seismic fracture characterization: SEG References No. 17.

Venstad, J. M., 2014, Dynamic time warping **-** An improved method for 4D and tomography time shift estimation?: Geophysics, **79**, no. 5, R209–R220. http://dx.doi.org/10.1190/geo2013-0239.1.